Published in final edited form as:
J Cell Physiol. 2009 July ; 220(1): 129–135. doi:10.1002/jcp.21740.

The subnuclear organization of histone gene regulatory proteins and 3′ end processing factors of normal somatic and embryonic stem cells is compromised in selected human cancer cell types

Prachi N. Ghule[1,2], **Zbigniew Dominski**[3], **Jane B. Lian**[1,2], **Janet L. Stein**[1,2], **Andre J. van Wijnen**[1,2], and **Gary S. Stein**[1,2,*]

[1] Center for Stem Cell Biology and Regenerative Medicine, University of Massachusetts Medical School, 55 Lake Avenue North, Worcester, MA 01655

[2] Department of Cell Biology and Cancer Center, University of Massachusetts Medical School, 55 Lake Avenue North, Worcester, MA 01655

[3] Program in Molecular Biology and Biotechnology, University of North Carolina at Chapel Hill, Chapel Hill, NC 27599, USA

Abstract

Human histone gene expression is controlled at the level of transcription initiation and subsequent 3′end processing to generate non-polyadenylated stem-loop containing histone mRNAs. Transcription is controlled at the G1/S phase transition by the Cyclin E/CDK2 mediated induction of $p220^{NPAT}$/HiNF-P complexes at subnuclear domains designated Histone Locus Bodies (HLBs) that associate with histone gene clusters. Histone mRNA maturation is mediated by Lsm10 containing U7snRNP complexes. In normal human somatic and embryonic stem cells, the 6p histone locus, the transcription marker $p220^{NPAT}$ and the 3′end processing marker Lsm10 (but not the Cajal Body marker coilin) co-localize, reflecting the assembly of an integrated factory for histone gene expression. Using in situ immuno-fluorescence microscopy and fluorescence in situ hybridization (FISH), we show that this subnuclear organization is compromised in some cancer cell lines. In aneuploid cells, the presence of Histone Locus Bodies correlates with the number of histone gene loci. More importantly, the in situ co-localization of $p220^{NPAT}$ and Lsm10 is disrupted in HeLa S3 cervical carcinoma cells and MCF7 breast adenocarcinoma cells, with most Lsm10 residing in Cajal Bodies. The finding that the subnuclear integration of transcriptional initiation and 3′end processing of histone gene transcripts is deregulated may be causally linked to tumor-related modifications in molecular pathways controlling histone gene expression during the cell cycle.

Keywords

cell cycle; histone; $p220^{NPAT}$; HiNF-P; Histone Locus Body; Cajal body; Lsm10; Lsm11; U7 snRNP; coilin; human embryonic stem cells

Introduction

Proliferation of normal diploid human cells is coupled with mitogen-related progression through the restriction (R) point in late G1 when cells attain competency for S phase

Address correspondence to: Gary S. Stein, Department of Cell Biology and Cancer Center, University of Massachusetts Medical School, 55 Lake Avenue North, Worcester, MA 01655, Tel: (508) 856-5625; Fax: (508) 856-6800; gary.stein@umassmed.edu.

initiation and progression (Pardee, 1974; Pardee, 1989). Cancer cells exhibit deregulation of the R point as reflected by reduced growth factor dependence but these cells must still temporally control the subsequent induction of DNA replication and human histone gene expression at the G1/S phase transcription. The transcriptional activation of multiple histone genes, which encode the highly conserved proteins that package newly replicated DNA as chromatin, represents a universal gene regulatory mechanism that is operative in both somatic and embryonic stem cells (Stein et al, 1996; Luong et al, 2002; Mitra et al, 2003; Miele et al, 2005; Braastad et al, 2004; Holmes et al, 2005; Becker et al, 2006; Becker et al, 2007; Medina et al, 2007; Medina et al, 2006).

In both human somatic and embryonic stem cells, the principal regulatory proteins that mediate human histone gene transcription are concentrated at specific subnuclear domains referred to as Histone Locus Bodies (Ghule et al, 2008). The histone gene co-activator protein $p220^{NPAT}$ (Nuclear Protein, ataxia-telangiectasia locus) is stimulated in late G1 by cyclin E/CDK2 dependent phosphorylation and subsequently recruited by the transcription factor HiNF-P (Histone Nuclear Factor-P) to histone H4 gene promoters (Zhao et al, 1998; Zhao et al, 2000; Ma et al, 2000; Ye et al, 2003; Wei et al, 2003; Mitra et al, 2003; Miele et al, 2005). Histone genes, HiNF-P and $p220^{NPAT}$ represent primary architectural components of Histone Locus Bodies. Nascent primary histone transcripts contain a unique 3′ stem-loop structure that binds Stem Loop Binding Protein (SLBP) (Wang et al, 1996). Cleavage of histone transcripts at the 3′end depends on U7 small nuclear ribonucleoprotein complexes (U7snRNPs) that contain several protein subunits, including Lsm10 (U7 snRNP-specific Sm-like protein 10) and Lsm11 (U7 snRNP-specific Sm-like protein 11) (Dominski and Marzluff, 2007; Pillai et al, 2001; Pillai et al, 2003; Dominski et al, 2003). U7snRNPs are thought to be assembled in Cajal Bodies, but the number of Cajal Bodies and the localization of 3′ processing factors varies in different cell types (Frey and Matera, 1995; Liu et al, 2006; White et al, 2007; Ghule et al, 2007; Bongiorno-Borbone et al, 2008). We have previously shown that in normal human somatic and embryonic stem cells, the transcriptional regulator $p220^{NPAT}$ and the 3′ processing marker Lsm10 co-localize in Histone Locus Bodies yet both proteins are less frequently present in coilin-containing Cajal Bodies (Ghule et al, 2008).

Deregulation of subnuclear organization is a hallmark of tumor cells (Stein et al, 2008; Zaidi et al, 2007) and a key question that remains to be addressed is whether the regulatory assembly of Histone Locus Bodies is altered in cancer cells due to deregulation of cell growth regulatory pathways. Here, we examined the micro-environment mediating histone gene transcription and processing in different cancer cell types to assess whether there are spatial differences in the nuclear organization of the machinery that produces histone gene transcripts in S phase. The principal finding is that the normal presence of Lsm10, $p220^{NPAT}$ and histone genes at Histone Locus Bodies is disrupted in at least two distinct cancer cell types where $p220^{NPAT}$ and Lsm10 now reside in distinct compartments. This architectural perturbation represents a functional and spatial separation between histone transcription and 3′ end processing that may reflect pathological molecular pathways that control cell growth of cancer cells.

Materials and Methods

Immunofluorescence (IF) Microscopy

IF microscopy was performed with panel of distinct human cell types (U2OS and SAOS-2 osteosarcoma cells, T98G glioblastoma cells, MDA-MB-231 and MCF7 breast adenocarcinoma cells, PC-3 prostate adenocarcinoma and HeLa S3 cervical carcinoma cells). Each cell type was propagated as recommended (www.atcc.com) and grown on gelatin coated coverslips for IF analysis. IF was carried out as described previously (Ghule

et al, 2007). Briefly, cells were fixed with 3.7% formaldehyde for 10 min, permeabilized by 0.25% Triton-X-100 for 20 min and then treated with primary antibody for 1 h at 37°C, followed by detection using appropriate fluorescent tagged secondary antibody. The nuclei were counter-stained with DAPI.

Antibodies, their working dilutions and their supplier are as follows: monoclonal $p220^{NPAT}$ (mouse monoclonal, 1:1000, BD Biosciences), polyclonal $p220^{NPAT}$ (rabbit polyclonal, 1:1000) (Ma et al, 2000; Zhao et al, 2000), coilin (pdelta) (mouse monoclonal, 1:500, Santa Cruz Biotech), coilin (rabbit polyclonal, 1:500, (Andrade et al, 1991)) and Lsm10 (mouse monoclonal, 1:500, Biomatrix Research). Secondary antibodies were goat anti-mouse Alexa 488, goat anti-rabbit Alexa 488, goat anti-mouse Alexa 594, goat anti-rabbit Alexa 594, goat anti-mouse Alexa 350, goat anti-rabbit Alexa 350 (all 1:800 dilution in 1X PBSA).

Fluorescence in Situ Hybridization (FISH)

Probes were made of BAC clones spanning a region very near to the major histone gene locus on chromosome 6p21 (RP11-2p4) (Children's Hospital Oakland Research institute, Oakland, CA). BAC DNA was purified using Qiagen columns and probe DNA was labeled using the DIG Nick translation kit (Cat# 11745816910 Roche Diagnostics, Indianapolis, IN) according to the manufacturer's protocol. The probe mixture was prepared by adding 50-100ng of probe DNA, 70% formamide, 10μg human Cot-1 DNA and 10μg salmon sperm DNA. FISH was performed after cells were subjected to IF as described above. After IF, cells were fixed by passing through ethanol grades (70%, 85% and 100%) and briefly air dried. Cells were then co-denatured with the probe mixture at 80°C for 8 min and allowed to hybridize overnight at 37°C in a moist chamber. Cells were washed using 50% formamide/ 4X SSC for 15 min at 37°C, followed by washes in 2X SSC 15 min at 37°C and 1X SSC 15 min at room temperature. Probes were detected by incubation with appropriate secondary antibody followed by 3 washes with 4X SSC, 0.1% Triton/4X SSC, and 4X SSC at room temperature with shaking. The secondary antibody used for FISH analysis was anti-DIG rhodamine (Roche) (1:500 in 4X SSC/1%BSA). Some cells then were counterstained with DAPI and mounted in Prolong-Gold (Invitrogen). Cells were viewed under an epifluorescence Zeiss Axioplan 2 microscope and images were captured using a Hamamatsu (C4742-95) charged coupled device (CCD) camera and analyzed by Metamorph imaging software (Universal Imaging). All images were captured with a 100x/1.4 Plan-Apochromat oil immersion objective.

Results

Aneuploidy related amplification of Histone Locus Bodies in multiple cancer cell types

In this study, we assessed the subnuclear organization of the histone gene expression machinery in different tumor-derived cell types for comparison with normal human diploid cells (e.g., WI38 fibroblasts and H9 embryonic stem cells). The cancer cell lines we used were U2OS and SAOS-2 osteosarcoma cells, T98G glioblastoma cells, MDA-MB-231 and MCF-7 breast adenocarcinoma cells, PC-3 prostatic adenocarcinoma cells and HeLa S3 cervical carcinoma cells. We examined the presence of the histone gene co-regulator $p220^{NPAT}$ (which forms an obligatory complex with histone H4 gene transcription factor HiNF-P) and Lsm10 (a major component of the U7 snRNP related to the 3′ end processing machinery) in Histone Locus Bodies (characterized by a nucleic acid probe recognizing 6p) or Cajal Bodies (based on its resident protein Coilin) (Fig. 1).

Unlike normal human diploid cells that typically have 2-4 Histone Locus Bodies containing the histone gene regulator $p220^{NPAT}$, all cancer cell types we examined contain 3 to 6 times that many Histone Locus Bodies (i.e., 6 to 18 $p220^{NPAT}$ foci per cell)(Fig. 1 and Table 1),

consistent with our previous observations (Ghule et al, 2007; Ghule et al, 2008). The number of Cajal Bodies is more variable and is consistently lower than the number of Histone Locus Bodies (ranging from 1 to 8 coilin foci per cell). The cancer cell lines we examined are all aneuploid and their genome content ranges in general from hypotriploid to hyperpentaploid. Thus, the aneuploid state of each cell type correlates to some extent with the number of Histone Locus Bodies and to a lesser extent with the number of Cajal Bodies.

While it is well-known that the various cancer cell lines we used exhibit aneuploidy, it is not exactly known to what extent these cell lines are polyploid for the major histone gene locus on chromosomal interval 6p21. Therefore, we examined the number of Histone Locus Bodies and Cajal Bodies in each of these cell lines in relation to a nucleic acid probe close to the 6p21 region by FISH. Our results show indeed that the number of 6p related sequences is increased in each of the cancer cell lines and that approximately one half of the $p220^{NPAT}$ foci that characterize Histone Locus Bodies are associated with 6p derived sequences (Fig. 1 and Table 1&2) (Note: the other half should localize with the 1q22 histone gene cluster). In contrast, coilin foci that reflect Cajal Bodies are not consistently associated with the histone cluster at 6p and only exhibit co-localization for a limited subset (Fig. 1 and Table 1&2). Hence, these data indicate that the number of Histone Locus Bodies is linked to the aneuploid state of cancer cells and that Cajal Bodies represent subnuclear domains that are less directly coupled to the in situ regulation of histone gene expression.

The subnuclear concentration of the 3′ end processing factor Lsm10 in Histone Locus Bodies is deregulated in selected cancer cell types

We have previously shown that the U7snRNP subunit Lsm10 that supports maturation of histone mRNA transcripts by 3′ end processing is invariably associated with $p220^{NPAT}$ foci in normal diploid human somatic and embryonic stem cells (Ghule et al, 2008). To understand if the functional organization of transcriptional and 3′ end processing components of the histone gene expression machinery in the same subnuclear compartment is retained in tumor cells, we assessed the localization of Lsm10 in relation to $p220^{NPAT}$ and coilin in our panel of cancer cell lines.

In the majority of these cell types (e.g., U2OS, SAOS-2, MDA-MB-231, T98G and PC-3), the 3′ end processing marker Lsm10 is invariably detected in the vicinity of 6p (Fig. 1). In the same cell types, the signals of Lsm10 and $p220^{NPAT}$ consistently overlap at Histone Locus Bodies (Fig. 2 and Table 2). Strikingly, Lsm10 is not consistently observed in the vicinity of the 6p histone cluster in HeLa S3 cells or MCF-7 cells (Fig. 1), nor do Lsm10 signals correlate with $p220^{NPAT}$. Instead, in both cell types, Lsm10 co-localizes with coilin at Cajal Bodies (Fig. 2 and Table 2). These results suggest that the localization of Lsm10 at $p220^{NPAT}$ foci and histone gene loci is deregulated in selected cancer cell types.

Dissociation of the 3′ end processing machinery from transcription initiation complexes at histone loci in distinct cancer cell types

Although there are clear distinctions in the localization of $p220^{NPAT}$, Lsm10 and coilin, we note that all three proteins do partially overlap in each of the cell lines and that the distribution and proximity of these factors is in part cell cycle dependent (Tables 1 and 2). For example, the number of $p220^{NPAT}$ foci at Histone Locus Bodies is twice the number of 6p loci, because these foci also form on the second major histone gene cluster on 1q. There is also variation in the size of Histone Locus Bodies, which is directly related to the larger size of 6p histone cluster relative to the 1q cluster. The detection of the smaller 1q histone gene cluster may be subject to threshold and may become more apparent as cells enter S phase. Additional variation in the size of Histone Locus Bodies may arise from cancer-related duplication of histone gene clusters, as has been observed in the organization of the

canonical human genome (Braastad et al, 2004). Furthermore, the number of Histone Locus Bodies varies by two fold as G2 cells exhibit twice the number of 6p histone loci after genome replication during S phase. Genomic heterogeneity in different cell types may also contribute to some variation in the detection of histone-related focal domains. In rare instances, we observe that $p220^{NPAT}$ foci do not co-localize with the 6p locus.

The number of Cajal Bodies is highly variable and only a subset of cells contains detectable coilin that concentrates in specific foci (~40-60% of cells) (Table 1). Occasionally, coilin signals merge with Lsm10 and $p220^{NPAT}$ signals (in 20-35% of cells), presumably as cells progress through late S (Ghule et al, 2008), suggesting that Cajal Bodies and Histone Locus Bodies may coalesce. Interestingly, in HeLa S3 and MCF-7 cells, we observe that 3′end processing factors localize at Cajal Bodies that are larger and more distinct than in other cell types. The significance of this observation remains unclear. Because of the variation in the spatial organization of $p220^{NPAT}$, Lsm10 and coilin foci and the 6p histone locus, we examined the multiple interrelationships in a large number of cells (n>100) and quantified the pairwise correlations between these parameters of histone gene expression as percentage overlap in our panel of seven cancer cell lines (Fig. 3). These quantitative analyses reaffirm the interpretation that the normal localization of Lsm10 with $p220^{NPAT}$ and the 6p histone locus is compromised in MCF-7 and HeLa S3 cells.

To test directly whether Lsm10 dissociates from Histone Locus Bodies in selected cancer cell types, we performed IF/FISH microscopy (simultaneously detecting two proteins and one DNA locus) of Lsm10, $p220^{NPAT}$ or coilin and the 6p histone locus. U2OS cells show normal association of Lsm10 with $p220^{NPAT}$ and the 6p locus as is observed in human ES and diploid somatic cells. In these cells Lsm10 is always associated with Histone Locus Bodies as indicated by almost 100% co-localization with $p220^{NPAT}$ and the 6p locus (Fig. 4 a,i&ii). In contrast to U2OS cells, HeLa S3 cells exhibit dissociation of Lsm10 from $p220^{NPAT}$ and 6p in most Histone Locus Bodies (Fig. 4 c&v). In these cells there is a clear distinction between $p220^{NPAT}$ and Lsm10 foci at the majority of HLBs (Fig. 4 c&v). However, IF/FISH analysis shows that in another subset (~20%), there is a clear three-way co-localization of $p220^{NPAT}$, Lsm10 and 6p (Fig. 4 c,vii). The association of between $p220^{NPAT}$, coilin and the 6p locus is significantly less frequent in both U2OS (~20%) and HeLa S3 (~20%) cells (Fig. 4 b&d). This three way co-localization is usually observed at only one of the Cajal Bodies (Fig. 4 b&d). Thus, the delocalization of Lsm10 is not absolute and there are apparently instances where all three components can interact together. We conclude that the deregulation in the localization of Lsm10 is a stochastic event rather than complete abrogation of the potential of Lsm10 to associate with Histone Locus Bodies.

Discussion

All cells must replicate their DNA during S phase, necessitating the expression of histone genes to package newly synthesized DNA into chromatin. We and others have previously shown that the machinery for histone gene expression is localized at specialized subnuclear domains, Histone Locus Bodies (Ghule et al, 2008; Frey and Matera, 1995; Liu et al, 2006; White et al, 2007; Ghule et al, 2007; Bongiorno-Borbone et al, 2008). In this study, we find that all aneuploid cancer cells examined have an increased number of $p220^{NPAT}$ foci that roughly correlates with increased copy number of the 6p derived histone gene locus. More importantly, we find that the strict spatial association of $p220^{NPAT}$ and Lsm10, which is observed in normal diploid human somatic and embryonic stem cells (Ghule et al, 2008), is sporadically deregulated in distinct cancer cell types.

The data presented in this paper clearly corroborate the now prevailing model that histone genes are not by necessity associated with coilin containing Cajal Bodies but instead

consistently localize to $p220^{NPAT}$ containing Histone Locus Bodies. The extent to which Cajal Bodies are associated with histone loci remains somewhat unclear. In normal somatic and embryonic stem cells, focal coilin staining is only observed in a limited number of cells (~20-50%). Studies with synchronized human embryonic stem cells suggest that Cajal Bodies are S/G2 phase related subnuclear domains (Ghule et al, 2007). Cajal Bodies represent locations where snRNP complexes are assembled (Ogg and Lamond, 2002; Gall, 2000). Association of Cajal Bodies in which large numbers of U7snRNPs are prepared for processing of histone primary transcripts with Histone Locus Bodies is thus beneficial for histone gene expression, but would only be expected to occur after sufficient numbers of primary transcripts have accumulated due to transcriptional activity.

One key question is why selected cancer cell types would exhibit this de-coupling between transcriptional components (e.g., $p220^{NPAT}$) and 3′ end processing components (e.g., Lsm10) that mediate histone gene expression in situ at Histone Locus Bodies. The normal sequestration of $p220^{NPAT}$ and Lsm10 optimizes the efficiency by which cells can produce histone mRNAs to respond promptly to demands in histone gene expression as DNA replication proceeds. This spatial arrangement is tightly regulated in situ at the transcriptional level by the Cyclin E/CDK2 dependent phosphorylation of the $p220^{NPAT}$/HiNF-P promoter complex (Miele et al, 2005; Zhao et al, 1998; Zhao et al, 2000; Ma et al, 2000). Transcription of histone genes may occur throughout the cell cycle as has been shown for selected human cancer cell types (e.g., HeLa S3) (Plumb et al, 1983; Baumbach et al, 1987) and mouse 3T6 fibroblasts (DeLisle et al, 1983). However, histone gene transcription could be deregulated by constitutive activation of the $p220^{NPAT}$/HiNF-P complex and/or promiscuous activation through HiNF-P independent mechanisms. Equally possible is the simultaneous deregulation of 3′ end processing mechanisms. The spatial sequestration of transcriptional and 3′ end processing mechanisms may normally support efficient S phase progression to the benefit of overall cell proliferation. However, the combined deregulation of both mechanisms would generate a futile cycle in which cells would unnecessarily produce and process histone primary transcripts that would then be degraded (due to lack of demand for histone proteins outside of S phase). Thus, it is plausible that the spatial organization of histone gene transcription and 3′ end processing factors in HeLa S3 cells and MCF-7 is compromised due to deregulation of the mechanisms that couple and activate these two processes in normal diploid cells.

Acknowledgments

We thank Bill Marzluff (University of North Carolina) and Wade Harper (Harvard Medical School) for generously providing antibodies and helpful suggestions of the manuscript. We thank the members of our laboratories for stimulating discussions, as well as Matthew Mandeville and Marissa Johnson for technical assistance. We also thank Judy Rask for assistance with manuscript preparation.

Contract Grant Sponsor: NIH; **Contract grant number**: R01 GM032010 and P01 CA082834 (to GSS) and RO1 GM058921 (to ZD). The contents of this manuscript are solely the responsibility of the authors and do not necessarily represent the official views of the National Institutes of Health.

References

Andrade LE, Chan EK, Raska I, Peebles CL, Roos G, Tan EM. Human autoantibody to a novel protein of the nuclear coiled body: immunological characterization and cDNA cloning of p80-coilin. J Exp Med. 1991; 173:1407–1419. [PubMed: 2033369]

Baumbach LL, Stein GS, Stein JL. Regulation of human histone gene expression: transcriptional and posttranscriptional control in the coupling of histone messenger RNA stability with DNA replication. Biochemistry. 1987; 26:6178–6187. [PubMed: 3689769]

Becker KA, Ghule PN, Therrien JA, Lian JB, Stein JL, van Wijnen AJ, Stein GS. Self-renewal of human embryonic stem cells is supported by a shortened G1 cell cycle phase. J Cell Physiol. 2006; 209:883–893. [PubMed: 16972248]

Becker KA, Stein JL, Lian JB, van Wijnen AJ, Stein GS. Establishment of histone gene regulation and cell cycle checkpoint control in human embryonic stem cells. J Cell Physiol. 2007; 210:517–526. [PubMed: 17096384]

Bongiorno-Borbone L, De Cola A, Vernole P, Finos L, Barcaroli D, Knight RA, Melino G, De Laurenzi V. FLASH and NPAT positive but not Coilin positive Cajal Bodies correlate with cell ploidy. Cell Cycle. 2008; 7:2357–2367. [PubMed: 18677100]

Braastad CD, Hovhannisyan H, van Wijnen AJ, Stein JL, Stein GS. Functional characterization of a human histone gene cluster duplication. Gene. 2004; 342:35–40. [PubMed: 15527963]

DeLisle AJ, Graves RA, Marzluff WF, Johnson LF. Regulation of histone mRNA production and stability in serum-stimulated mouse 3T6 fibroblasts. Mol Cell Biol. 1983; 3:1920–1929. [PubMed: 6656760]

Dominski Z, Marzluff WF. Formation of the 3′ end of histone mRNA: getting closer to the end. Gene. 2007; 396:373–390. [PubMed: 17531405]

Dominski Z, Yang XC, Kaygun H, Dadlez M, Marzluff WF. A 3′ exonuclease that specifically interacts with the 3′ end of histone mRNA. Mol Cell. 2003; 12:295–305. [PubMed: 14536070]

Frey MR, Matera G. Coiled bodies contain U7 small nuclear RNA and associate with specific DNA sequences in interphase human cells (erratum in: Proc Natl Acad Sci U S A 1995 Aug 29;92(18): 8532). Proc Natl Acad Sci USA. 1995; 92:5915–5919. [PubMed: 7597053]

Gall JG. Cajal bodies: the first 100 years. Annu Rev Cell Dev Biol. 2000; 16:273–300. [PubMed: 11031238]

Ghule PN, Becker KA, Harper JW, Lian JB, Stein JL, van Wijnen AJ, Stein GS. Cell cycle dependent phosphorylation and subnuclear organization of the histone gene regulator p220^{NPAT} in human embryonic stem cells. J Cell Physiol. 2007; 213:9–17. [PubMed: 17520687]

Ghule PN, Dominski Z, Yang XC, Marzluff WF, Becker KA, Harper JW, Lian JB, Stein JL, van Wijnen AJ, Stein GS. Staged assembly of histone gene expression machinery at subnuclear foci in the abbreviated cell cycle of human embryonic stem cells. Proc Natl Acad Sci U S A. 2008; 105:16964–16969. [PubMed: 18957539]

Holmes WF, Braastad CD, Mitra P, Hampe C, Doenecke D, Albig W, Stein JL, van Wijnen AJ, Stein GS. Coordinate control and selective expression of the full complement of replication-dependent histone H4 genes in normal and cancer cells. J Biol Chem. 2005; 280:37400–37407. [PubMed: 16131487]

Liu JL, Murphy C, Buszczak M, Clatterbuck S, Goodman R, Gall JG. The Drosophila melanogaster Cajal body. J Cell Biol. 2006; 172:875–884. [PubMed: 16533947]

Luong MX, van der Meijden CM, Xing D, Hesselton R, Monuki ES, Jones SN, Lian JB, Stein JL, Stein GS, Neufeld EJ, van Wijnen AJ. Genetic ablation of the CDP/Cux protein C terminus results in hair cycle defects and reduced male fertility. Mol Cell Biol. 2002; 22:1424–1437. [PubMed: 11839809]

Ma T, Van Tine BA, Wei Y, Garrett MD, Nelson D, Adams PD, Wang J, Qin J, Chow LT, Harper JW. Cell cycle-regulated phosphorylation of p220(NPAT) by cyclin E/Cdk2 in Cajal bodies promotes histone gene transcription. Genes Dev. 2000; 14:2298–2313. [PubMed: 10995387]

Medina R, van der Deen M, Miele-Chamberland A, Xie RL, van Wijnen AJ, Stein JL, Stein GS. The HiNF-P/p220^{NPAT} cell cycle signaling pathway controls non-histone target genes. Cancer Res. 2007; 67:10334–10342. [PubMed: 17974976]

Medina R, van Wijnen AJ, Stein GS, Stein JL. The histone gene transcription factor HiNF-P stabilizes its cell cycle regulatory co-activator p220^{NPAT}. Biochemistry. 2006; 45:15915–15920. [PubMed: 17176114]

Miele A, Braastad CD, Holmes WF, Mitra P, Medina R, Xie R, Zaidi SK, Ye X, Wei Y, Harper JW, van Wijnen AJ, Stein JL, Stein GS. HiNF-P directly links the cyclin E/CDK1/p220^{NPAT} pathway to histone H4 gene regulation at the G1/S phase cell cycle transition. Mol Cell Biol. 2005; 25:6140–6153. [PubMed: 15988025]

Mitra P, Xie RL, Medina R, Hovhannisyan H, Zaidi SK, Wei Y, Harper JW, Stein JL, van Wijnen AJ, Stein GS. Identification of HiNF-P, a key activator of cell cycle controlled histone H4 genes at the onset of S phase. Mol Cell Biol. 2003; 23:8110–8123. [PubMed: 14585971]

Ogg SC, Lamond AI. Cajal bodies and coilin--moving towards function. J Cell Biol. 2002; 159:17–21. [PubMed: 12379800]

Pardee AB. A restriction point for control of normal animal cell proliferation. Proc Natl Acad Sci U S A. 1974; 71:1286–1290. [PubMed: 4524638]

Pardee AB. G1 events and regulation of cell proliferation. Science. 1989; 246:603–608. [PubMed: 2683075]

Pillai RS, Grimmler M, Meister G, Will CL, Luhrmann R, Fischer U, Schumperli D. Unique Sm core structure of U7 snRNPs: assembly by a specialized SMN complex and the role of a new component, Lsm11, in histone RNA processing. Genes Dev. 2003; 17:2321–2333. [PubMed: 12975319]

Pillai RS, Will CL, Luhrmann R, Schumperli D, Muller B. Purified U7 snRNPs lack the Sm proteins D1 and D2 but contain Lsm10, a new 14 kDa Sm D1-like protein. EMBO J. 2001; 20:5470–5479. [PubMed: 11574479]

Plumb M, Stein J, Stein G. Coordinate regulation of multiple histone mRNAs during the cell cycle in HeLa cells. Nucleic Acids Res. 1983; 11:2391–2410. [PubMed: 6304651]

Stein GS, Stein JL, van Wijnen AJ, Lian JB. Transcriptional control of cell cycle progression: the histone gene is a paradigm for the G1/S phase and proliferation/differentiation transitions. Cell Biol Int. 1996; 20:41–49. [PubMed: 8936406]

Stein GS, Zaidi SK, Stein JL, Lian JB, van Wijnen AJ, Montecino M, Young DW, Javed A, Pratap J, Choi JY, Ali SA, Pande S, Hassan MQ. Genetic and epigenetic regulation in nuclear microenvironments for biological control in cancer. J Cell Biochem. 2008; 104:2016–2026. [PubMed: 18615590]

Wang ZF, Whitfield ML, Ingledue TC 3, Dominski Z, Marzluff WF. The protein that binds the 3′ end of histone mRNA: a novel RNA- binding protein required for histone pre-mRNA processing. Genes Dev. 1996; 10:3028–3040. [PubMed: 8957003]

Wei Y, Jin J, Harper JW. The cyclin E/Cdk2 substrate and Cajal body component p220(NPAT) activates histone transcription through a novel LisH-like domain. Mol Cell Biol. 2003; 23:3669–3680. [PubMed: 12724424]

White AE, Leslie ME, Calvi BR, Marzluff WF, Duronio RJ. Developmental and cell cycle regulation of the Drosophila histone locus body. Mol Biol Cell. 2007; 18:2491–2502. [PubMed: 17442888]

Ye X, Wei Y, Nalepa G, Harper JW. The cyclin E/Cdk2 substrate p220(NPAT) is required for S-phase entry, histone gene expression, and Cajal body maintenance in human somatic cells. Mol Cell Biol. 2003; 23:8586–8600. [PubMed: 14612403]

Zaidi SK, Young DW, Javed A, Pratap J, Montecino M, van WA, Lian JB, Stein JL, Stein GS. Nuclear microenvironments in biological control and cancer. Nat Rev Cancer. 2007; 7:454–463. [PubMed: 17522714]

Zhao J, Dynlacht B, Imai T, Hori T, Harlow E. Expression of NPAT, a novel substrate of cyclin E-CDK2, promotes S- phase entry. Genes Dev. 1998; 12:456–461. [PubMed: 9472014]

Zhao J, Kennedy BK, Lawrence BD, Barbie DA, Matera AG, Fletcher JA, Harlow E. NPAT links cyclin E-Cdk2 to the regulation of replication-dependent histone gene transcription. Genes Dev. 2000; 14:2283–2297. [PubMed: 10995386]

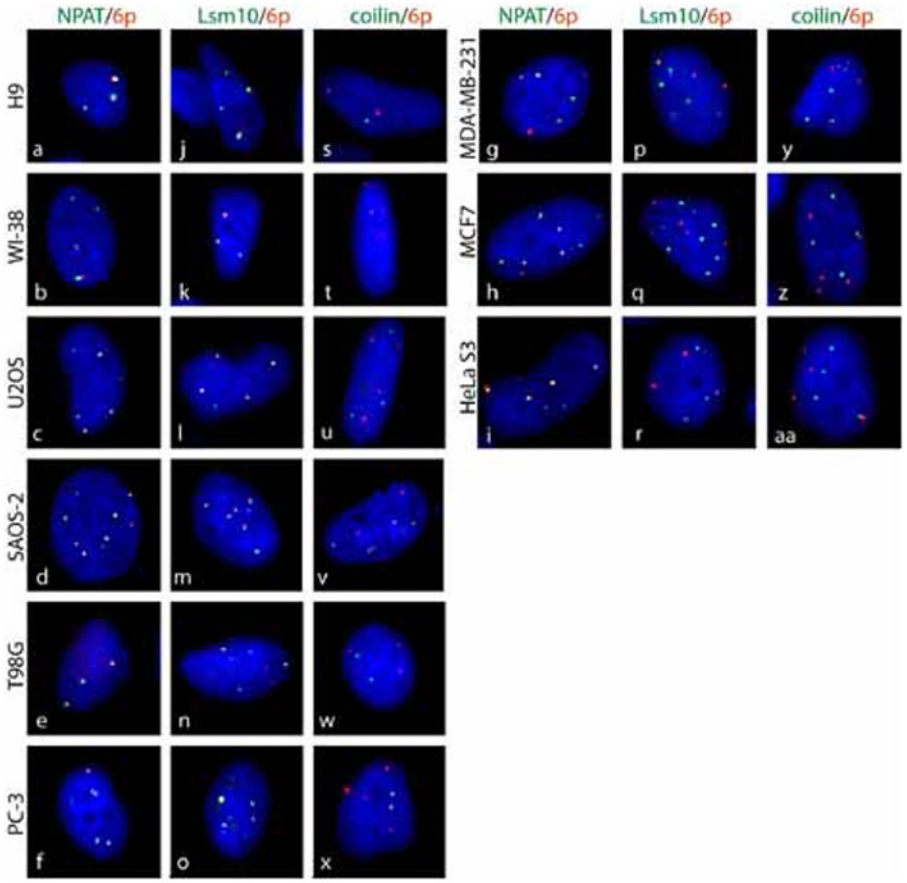

Figure 1. Amplification of number p220 ^{NPAT} (HLBs) foci is related to the change in copy number of histone locus

IF microscopy images were obtained using antibodies against p220^{NPAT} (green), or coilin (green) or Lsm10 (green) and a DIG-labeled FISH probe which hybridizes to 6p22 adjacent to the histone gene cluster on 6p21 (red). DAPI staining (blue) is used to visualize the nucleus. There are typically 6-18 p220^{NPAT} foci approximately half of which are consistently in proximity to histone gene clusters in all cancer cell types (panels a-i); the other half should colocalize with the histone gene locus on 1q22. Lsm10, the U7 snRNP component is associated with histone locus in some in H9, WI-38, U2OS, SAOS-2, T98G, PC3 and MDA-MB231 (panels: j-p) but not in HeLa S3 and MCF7 (panels: q, r) cells. In all these cancer cell types coilin foci (Cajal bodies) rarely are in proximity of Histone locus (panels: s-z, aa).

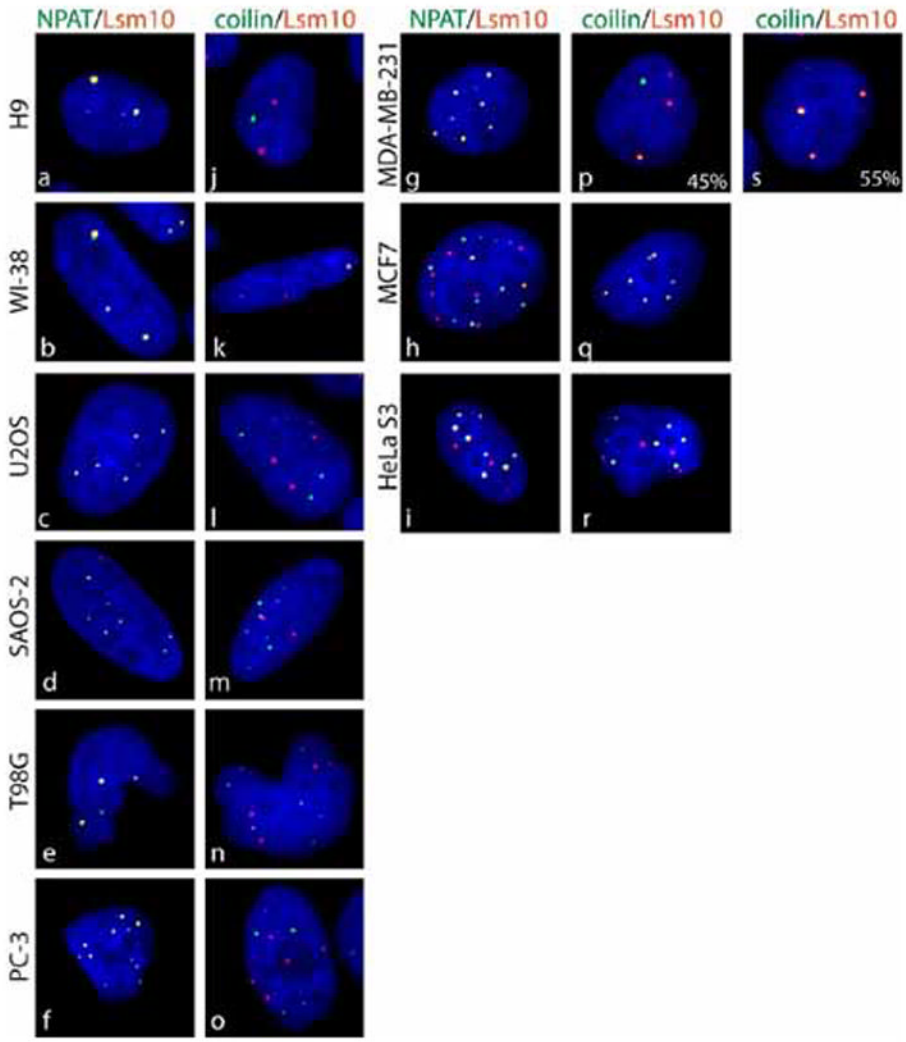

Figure 2. Localization of the 3′ end processing factor of histone mRNA Lsm10 in Histone Locus Bodies is deregulated in selected cancer cell types

IF microscopy images were obtained for different cancer cell types using antibodies against $p220^{NPAT}$ (green) or coilin (green) and one of the components of U7snRNP that process histone transcripts Lsm10(red). In normal cells and most cancer cell types (H9, WI-38, U2OS, SAOS-2, T98G, PC3) (panels: c-f) $p220^{NPAT}$ foci are associated with Lsm10 and not with Cajal bodies. In a subset of MDA-MB231 cells (panels: g,p,s) there is an intermediate phenotype where $p220^{NPAT}$ foci are associated with Lsm10 (~45%) while in the remainder Lsm10 is associated with coilin(~55%). In contrast, in ~80% of HeLa S3 and MCF7 cells Lsm10 is more frequently associated with coilin foci than with $p220^{NPAT}$ foci (panels: h,i,q,r).

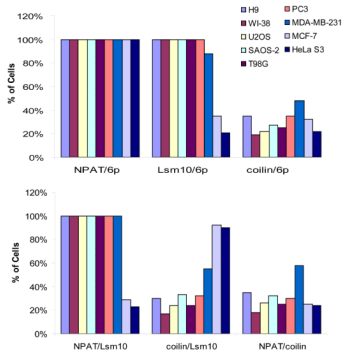

Figure 3. Relative distribution of Lsm10 in Histone Locus Bodies and Cajal Bodies

The graphs show quantitative analysis of the distribution of Lsm10 with respect to Histone Locus Bodies (as denoted by $p220^{NPAT}$ foci and histone gene clusters at 6p) versus Cajal Bodies (denoted by coilin foci). The micrographs represent the distribution of the association between these subnuclear domains in different normal and cancer cell types. To calculate the percentages, >100 cells were counted for each cell type.

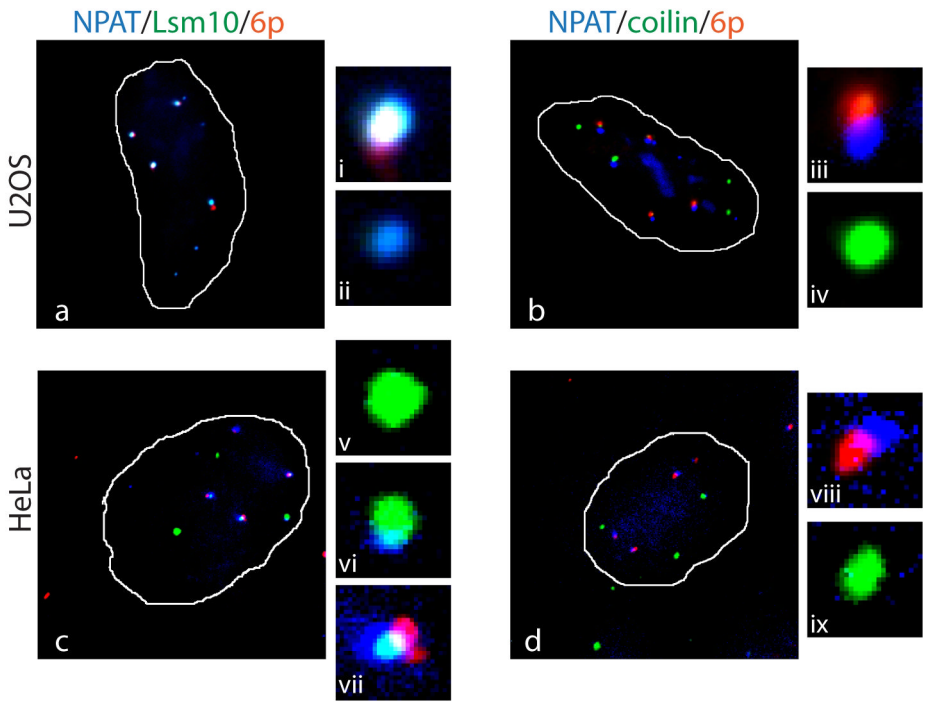

Figure 4. Dissociation of the 3′ end processing machinery of histone mRNA from p220^{NPAT} foci in distinct cancer cell types

IF microscopy for either Lsm10 (green) or coilin (green) with p220^{NPAT} (blue) and FISH for the 6p histone gene locus (red) was performed simultaneously using triple labeling. In U2OS cells, Lsm10 is associated with Histone Locus bodies and not with coilin foci (Panels a, b). In HeLa cells Lsm10 and coilin do not stain the same subnuclear domains as histone locus bodies as indicated by the arrows (Panels c & d). The small insets (i-ix) represent magnified images of the different focal organizations observed between Histone Locus Bodies (p220^{NPAT} & 6p locus) and Lsm10 foci or Cajal bodies.

Table 1

Distribution of Histone Locus Bodies and Cajal Bodies in Normal and Cancer Cell Types

The genome content of all cell lines as provided by the American Type Culture Collection (www.atcc.org) was correlated with the number of histone loci and foci for the indicated proteins. Histone Locus Bodies (HLB) are defined by the number of $p220^{NPAT}$ foci which are associated with the two major histone clusters (6p21 and1q22); thus, the number of HLBs is ~2fold the number of 6p loci. Lsm10 was used as a marker for U7 snRNPs and coilin as a marker for Cajal bodies. At least 100 cells were analyzed for each cell type.

Cell line	Genome content	6p Foci	NPAT foci (HLB)	Lsm10 foci	Coilin foci (CB)	Coilin positive cells
H9	diploid	2	2-4	2-4	1-3	50-60%
WI-38	diploid	2	2-4	2-4	1-3	12-15%
MDA-MB-231	near triploid	2-5	10-12	10-12	1-8	55-60%
PC-3	near triploid	3-6	8-18	8-18	1-6	45-50%
SAOS-2	hypotriploid	2-5	6-8	6-8	1-5	40-50%
U2OS	hypertriploid	2-4	6-8	6-8	1-5	40-50%
T98G	hyperpentaploid	2-5	6-10	6-10	1-3	40-50%
MCF-7	hypertriploid to hypotetraploid	4-5	8-10	7-12	1-8	70-75%
HeLa S3	aneuploid	3-4	8-10	7-12	2-8	75-80%

Table 2

Localization of Transcriptional components and 3′ End Processing Factors Relative to Histone Locus Bodies and Cajal Bodies

The overall spatial association of Histone Locus Bodies ($p220^{NPAT}$ foci), Lsm10 foci, Cajal bodies and histone gene clusters was determined by analyzing >100 cells per cell type.

A: Normal and Cancer Cell Types (H9, WI38, U2OS, SAOS2, T98G, PC3, MDA-MB-231)

	Histone Locus Bodies (NPAT)	Cajal Bodies (Coilin)	3′ End Processing Factors (Lsm10)	Histone Locus (6p21)
NPAT foci	-	Partial	Complete	Complete
Coilin foci	Partial	-	Partial	Partial
Lsm10 foci	Complete	Partial	-	Complete

B: Selected Cancer Cell Types HeLa S3/MCF7

	Histone Locus Bodies (NPAT)	Cajal Bodies (Coilin)	3′ End Processing Factors (Lsm10)	Histone Locus (6p21)
NPAT foci	-	Partial	Partial	Complete
Coilin foci	Partial	-	Complete	Partial
Lsm10	Partial	Complete	-	Partial